Interannual-to-Decadal Variability in the Bifurcation of the North Equatorial Current off the Philippines

B. Qiu and S. Chen

Dept of Oceanography, University of Hawaii

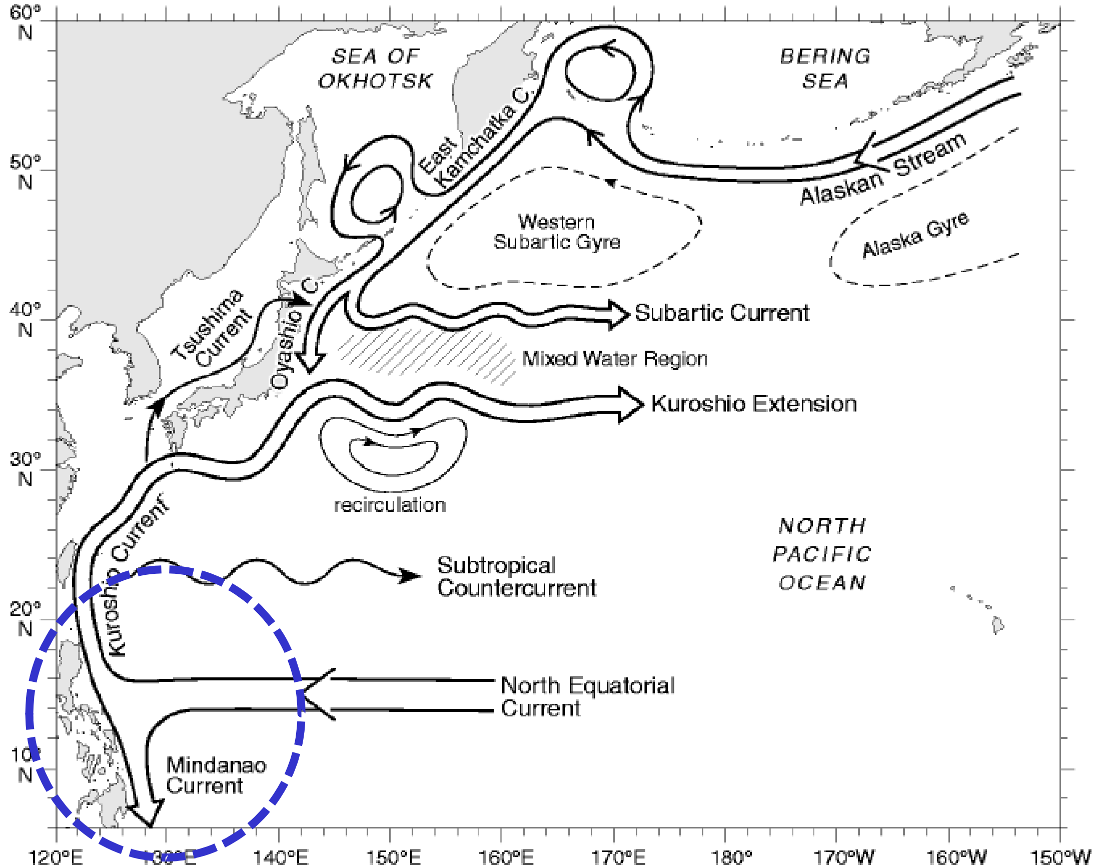

Western N Pacific circulation schematic

Importance of low-latitude western boundary current variability

Partitioning of NEC into Kuroshio and Mindanao Current

Conduit for midlat-origin T/S anomalies to equator

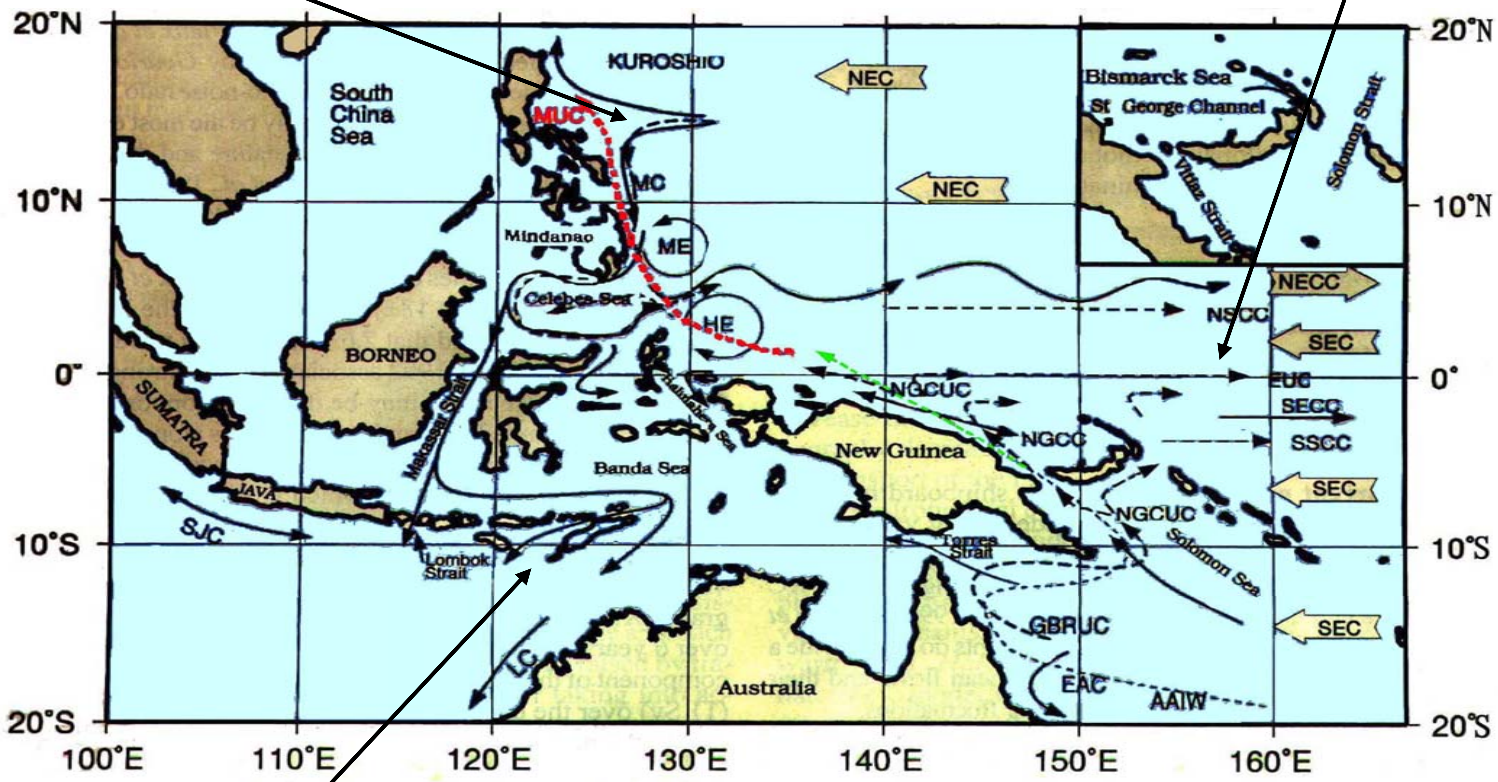

Impact on ITF transport and properties

Fine et al. (1994, JGR)

Mean SSH field in the western NP Ocean (Rio et al. 2009)

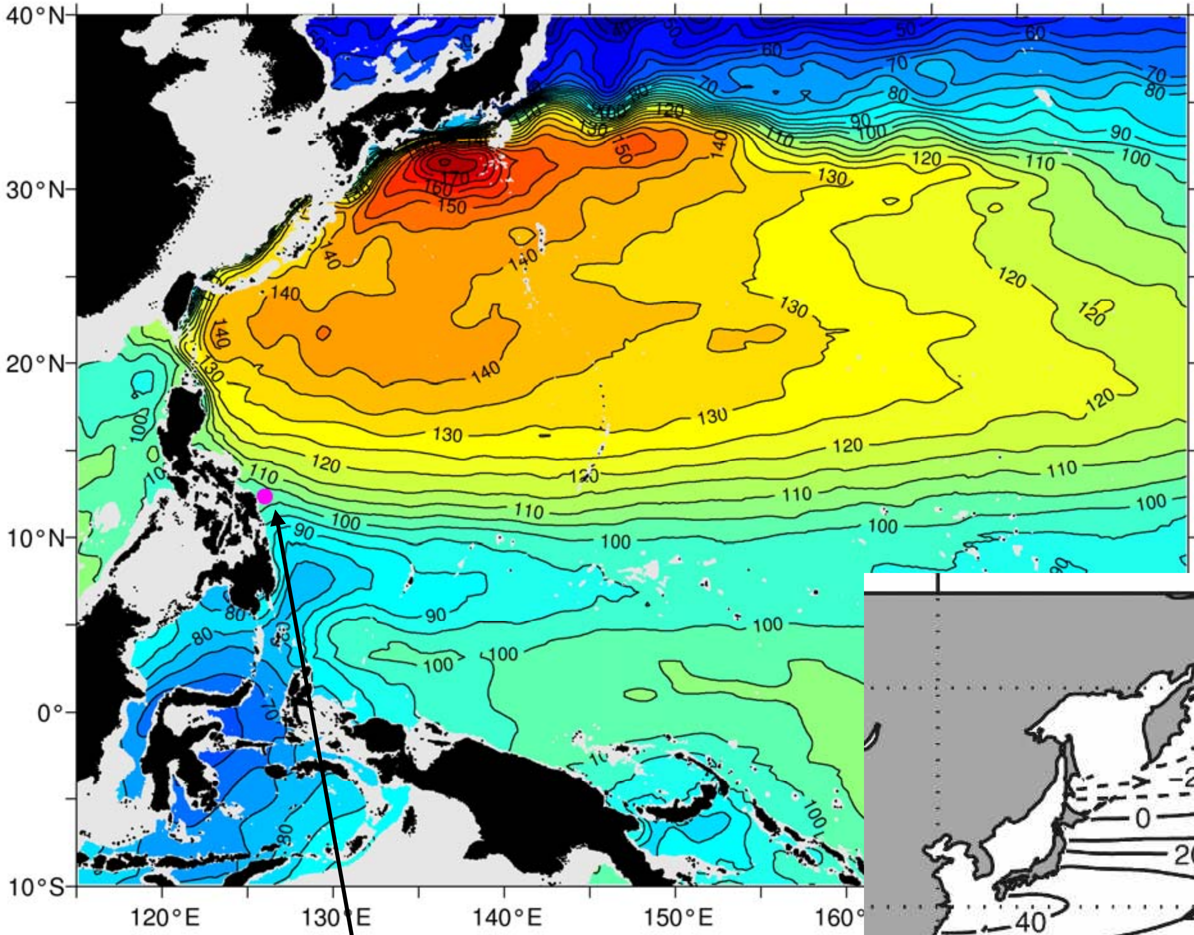

QuikSCAT Sverdrup streamfunction (Risien and Chelton 2008)

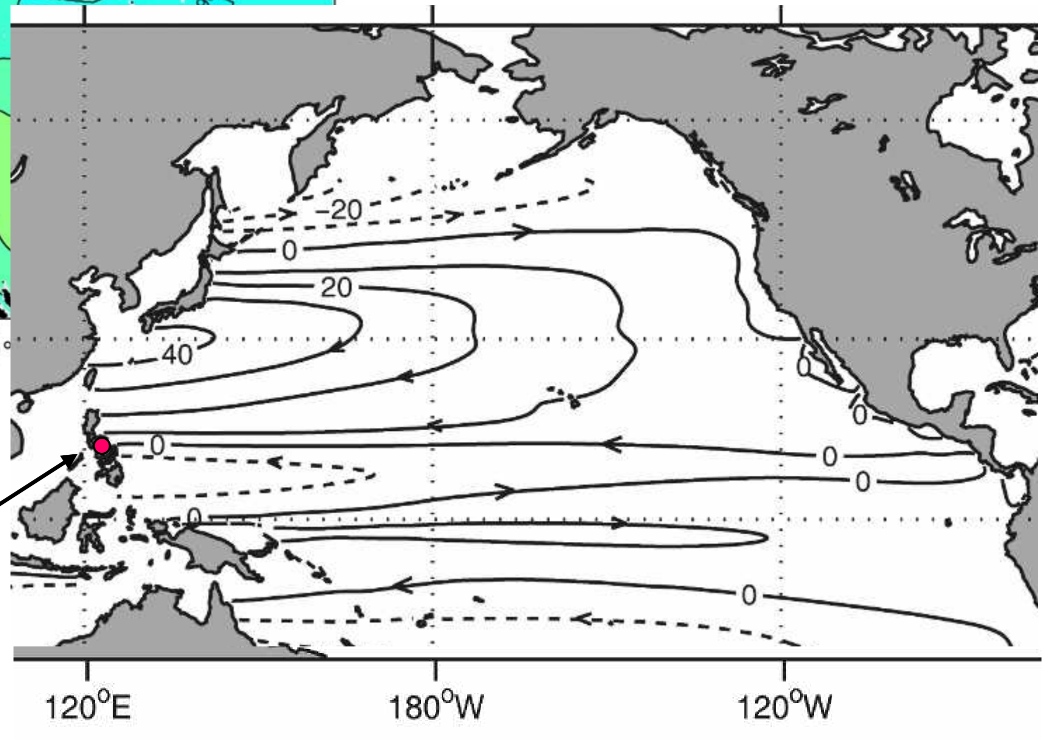

mean NEC bif. latitude

Large basin-scale seasonal migration in zero wind stress curl line

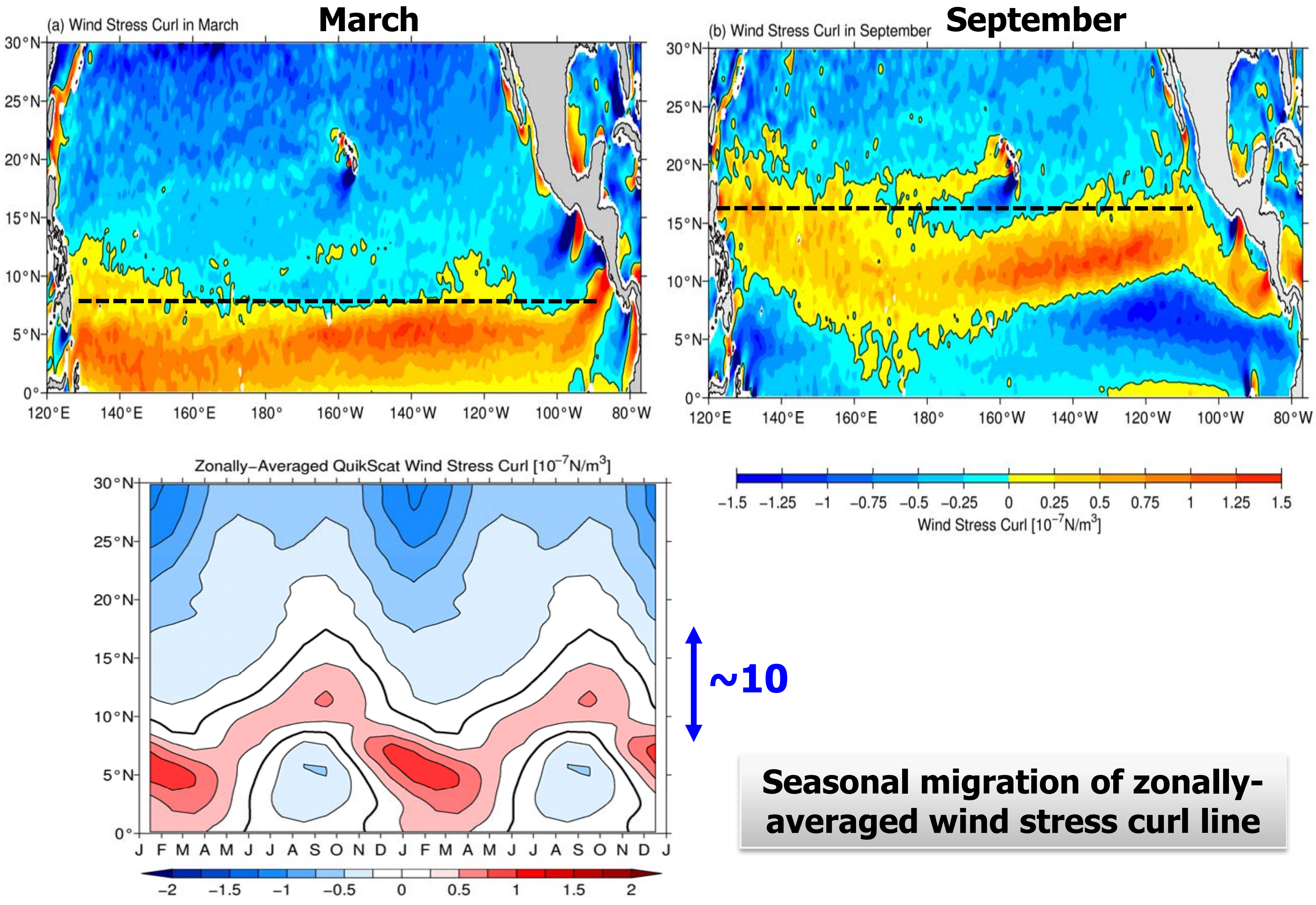

Seasonal migration of zonally-averaged wind stress curl line

Identifying time-varying NEC bifurcation along the Philippine coast

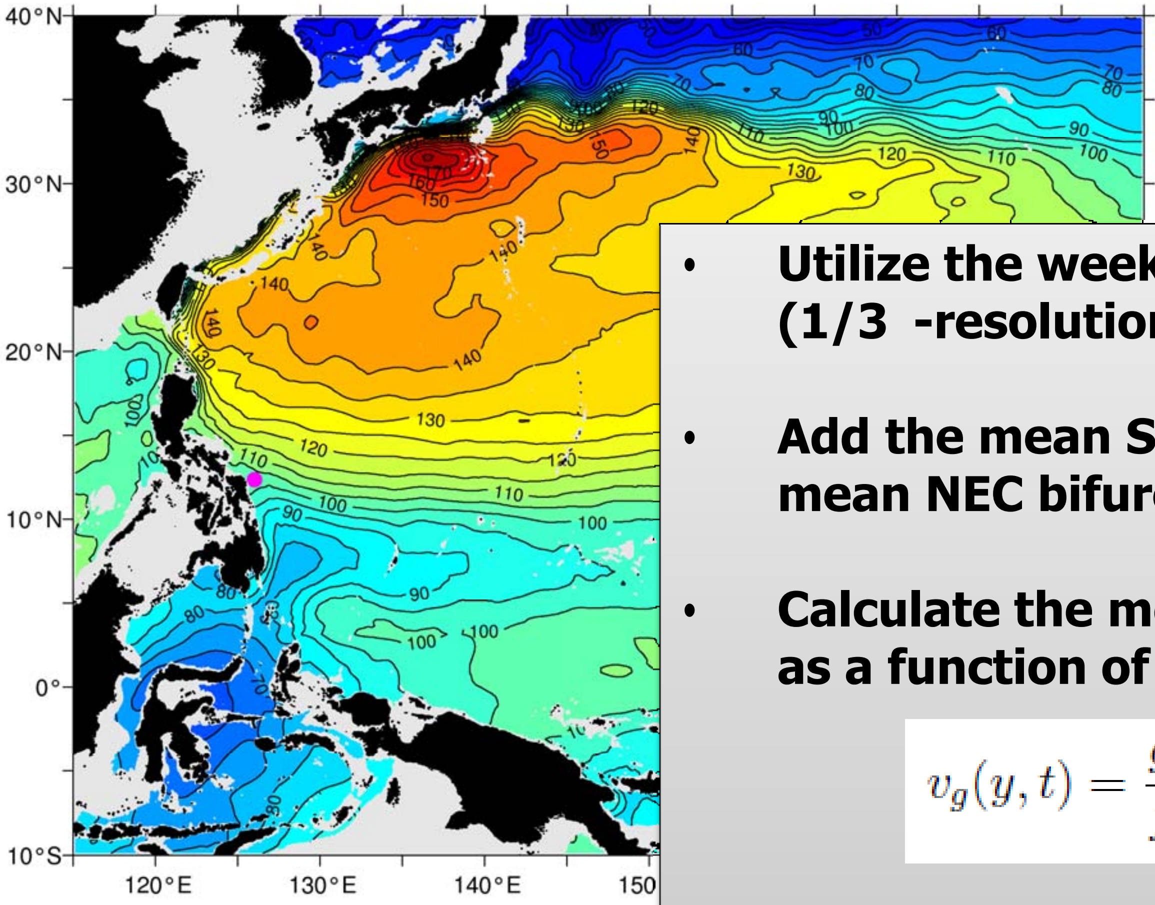

- **Utilize the weekly AVISO SSH anomaly data (1/3 -resolution, 10/1992-present)**

- **Add the mean SSH field of Rio et al. (2009): mean NEC bifurcation at ~12 N**

- **Calculate the meridional geostrophic velocity as a function of y along the Philippine coast:**

$$v_g(y,t) = \frac{g}{f}\left[h_e(y,t) - h_w(y,t)\right],$$

where h_e is SSH in 1 -band east of the coast and h_w in 1 -band further to the east

- **The NEC bifurcation latitude $Y_b(t)$ is defined at where v_g=0 in each month**

Time-varying NEC bifurcation inferred from AVISO SSH data

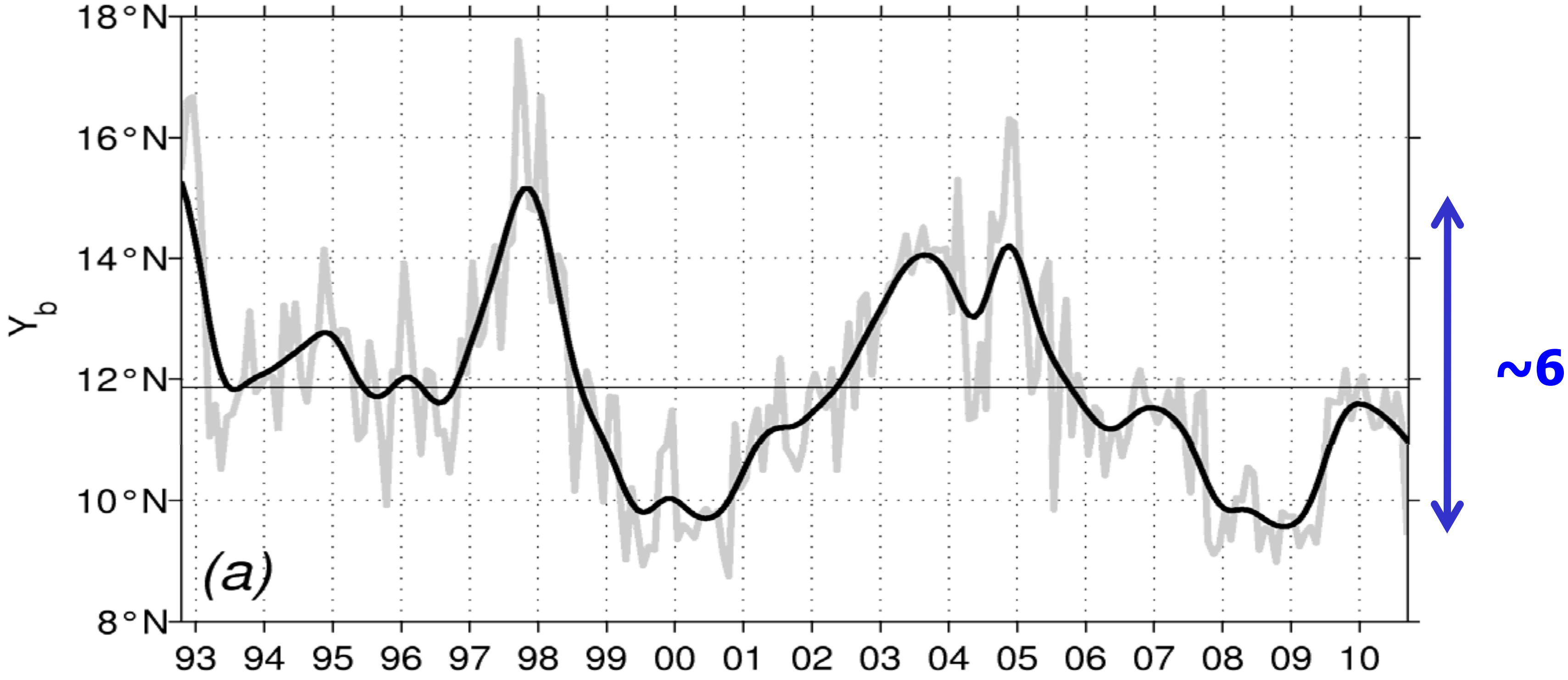

- **Presence of intraseasonal signals associated with the intrinsic MC variability**
- **Large migration on interannual-to-decadal time-scales**

SSH patterns in southerly vs. northerly bifurcation years

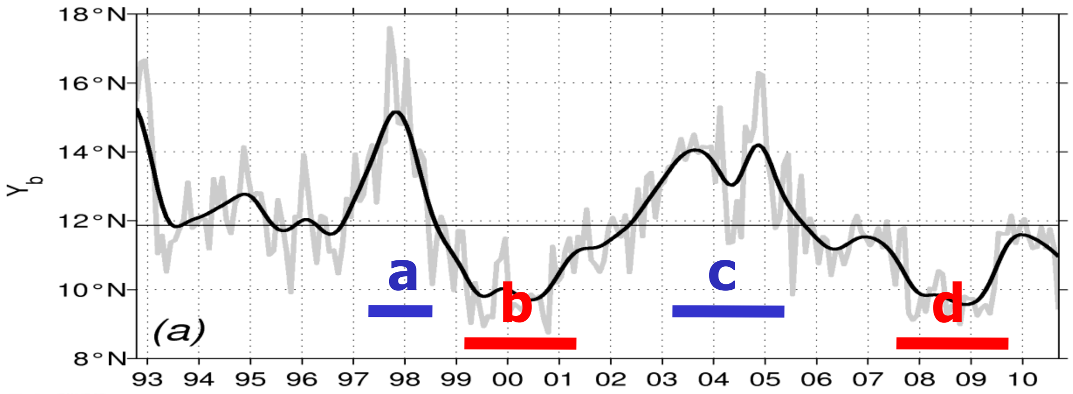

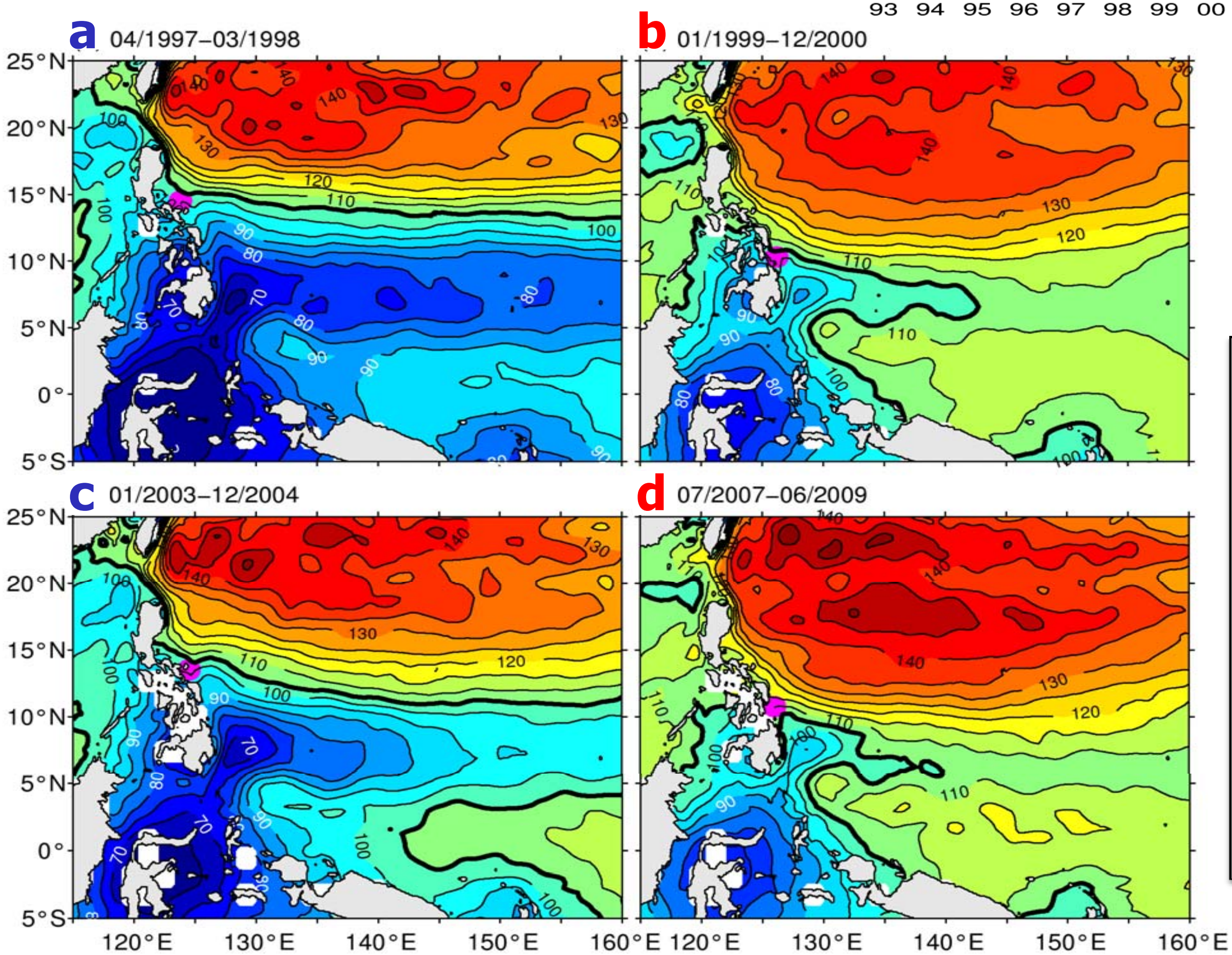

When Yb is northerly:

- **Better-defined thermocline ridge along 7 ~8 N**
- **Stronger Kuroshio and Mindanao C.**
- **Lower SSH in Sulu, Celebes, South China, and Indonesian Seas**

Linear correlation between $Y_b(t)$ and the local SSH time series

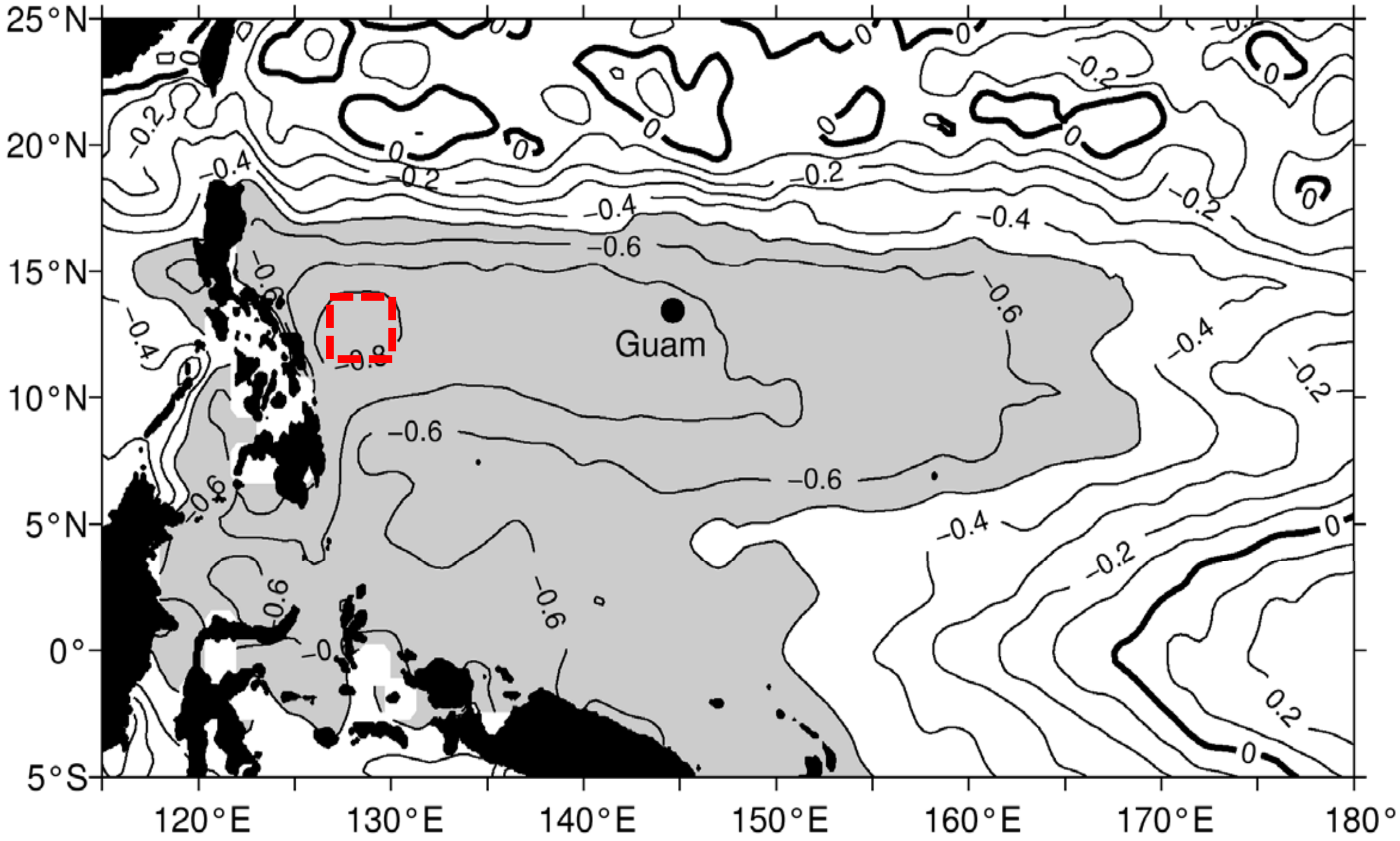

Given the high correlation, the observed SSH signals in the 12 -14 N and 127 -130 E box can be used as a proxy for $Y_b(t)$:

$$Y_p(t) = 11.9 - 0.13 \times h'(t) \quad (°\text{N}),$$

Proxy bifurcation latitude time series vs. $Y_b(t)$

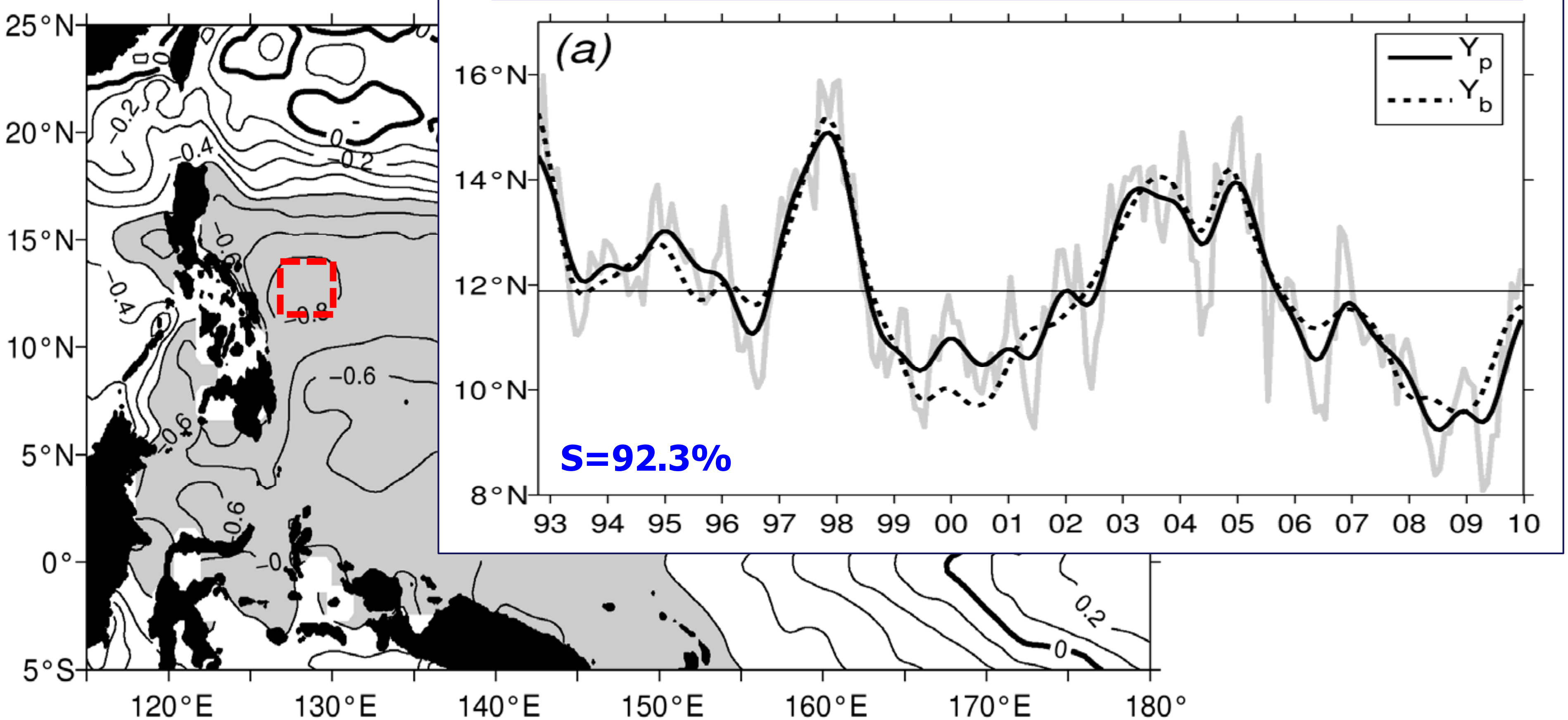

Given the high correlation, the observed SSH signals in the 12 -14 N and 127 -130 E box can be used as a proxy for $Y_b(t)$:

$$Y_p(t) = 11.9 - 0.13 \times h'(t) \quad (°\mathrm{N}),$$

Low-frequency SSH variability vs. wind stress curl forcing

- **Under the long-wave approximation, large-scale SSH changes are governed by linear vorticity dynamics:**

$$\boxed{\frac{\partial h'}{\partial t} - c_R \frac{\partial h'}{\partial x} = -\frac{g' \, \mathrm{curl}\, \boldsymbol{\tau}}{\rho_o g f} - \epsilon h',}$$

- **Given the wind forcing, SSH changes can be found by integrating the above equation along the Rossby wave characteristics:**

$$\boxed{h'_m(x,y,t) = \frac{g'}{\rho_o g f} \int_{x_e}^{x} \frac{1}{c_R} \mathrm{curl}\, \boldsymbol{\tau} \left(x', y, t + \frac{x - x'}{c_R} \right) \exp\left[\frac{\epsilon}{c_R}(x - x') \right] dx',}$$

c_R **: observed value**

$\mathrm{curl}\, \boldsymbol{\tau}$ **: monthly ECMWF reanalysis data (Balmaseda et al. 2008)**

ϵ **: Newtonian damping rate (=1/2 yrs.)**

x-t plot of observed vs. modeled SSH anomalies along 12°-14°N

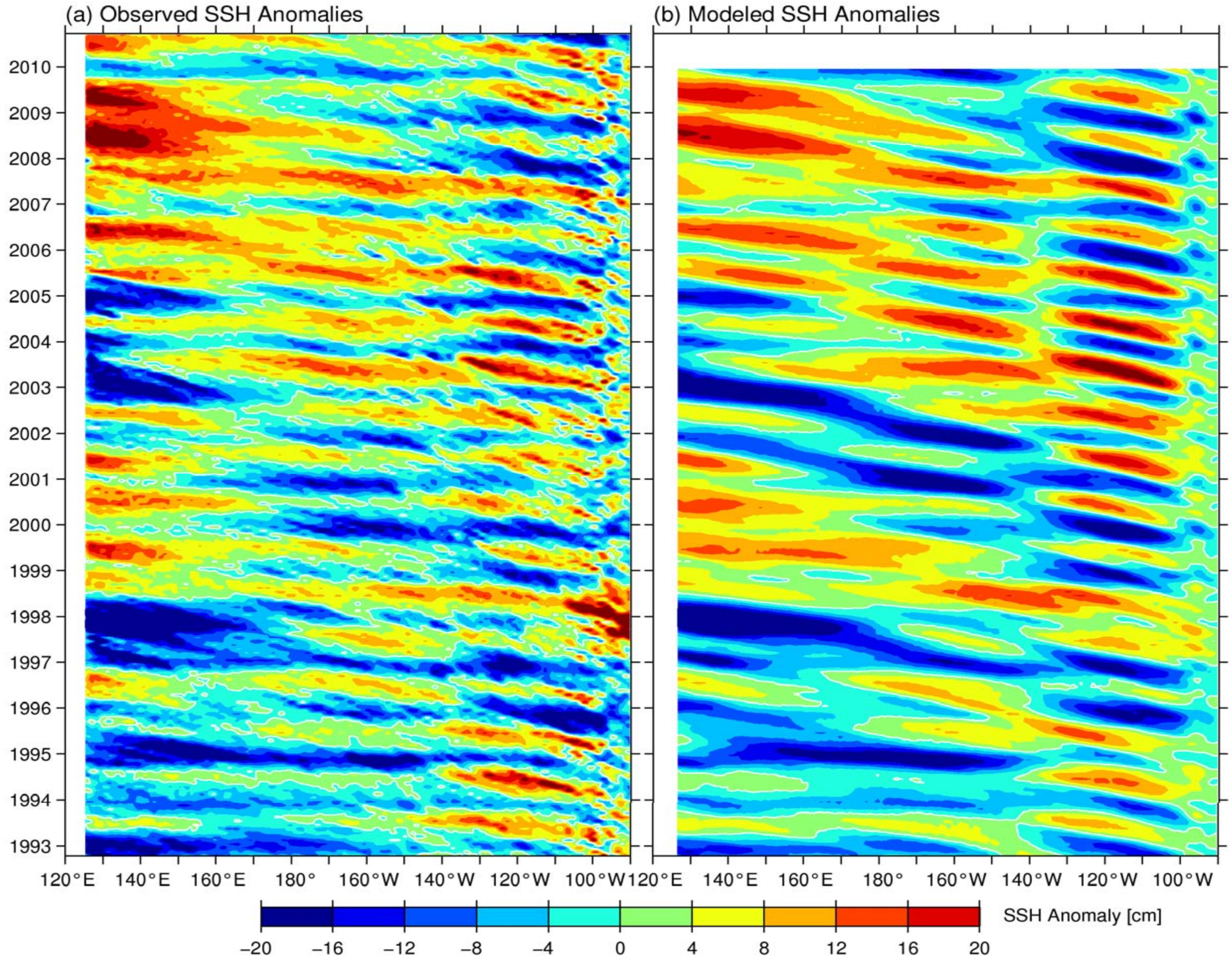

Proxy bifurcation latitudes from observed vs. modeled SSH data

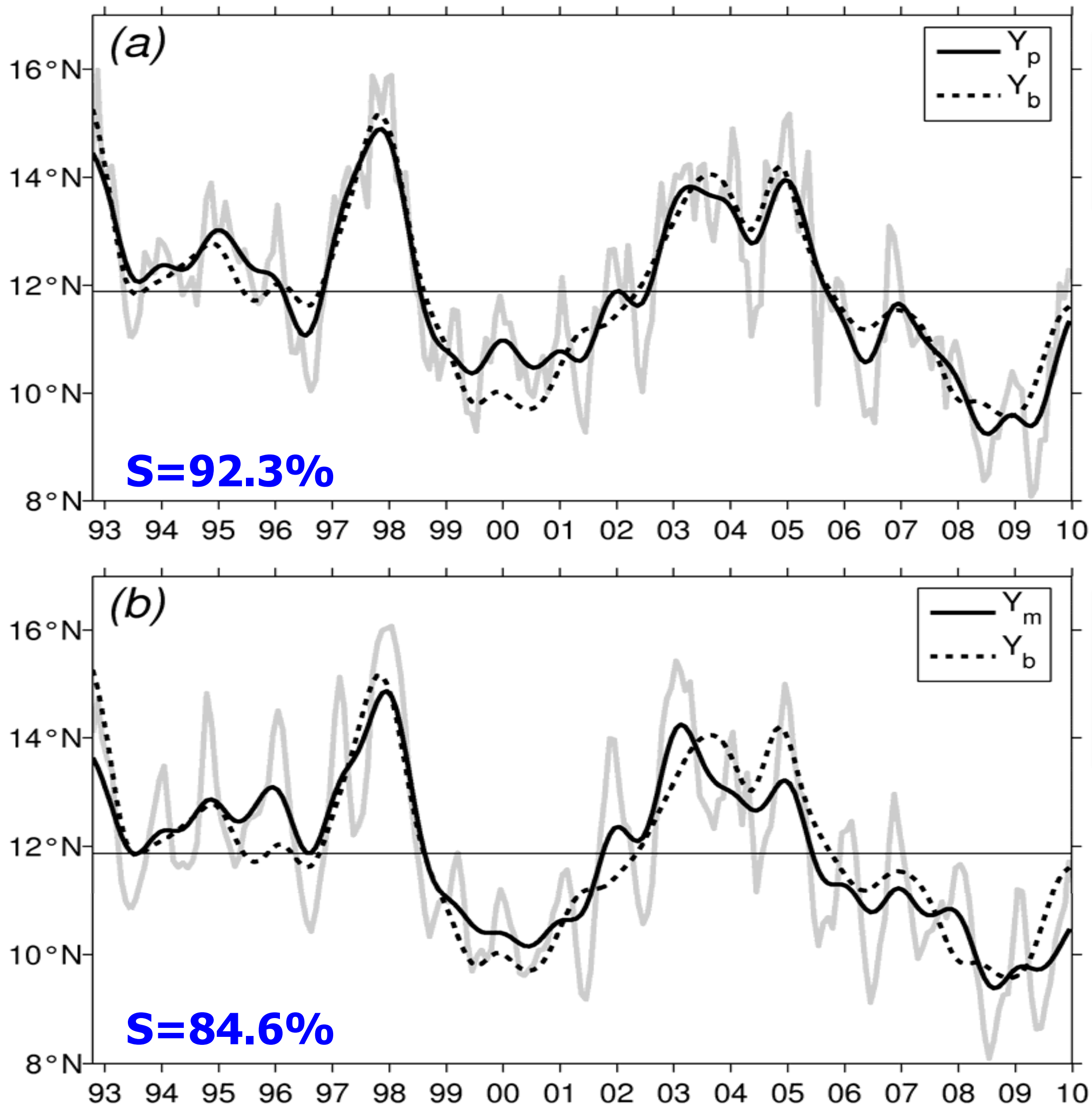

Proxy Y_p using observed SSH signals in the 12 - 14 N, 127 -130 E box

Proxy Y_m using modeled SSH signals in the 12 - 14 N, 127 -130 E box

Dashed lines: observed $Y_b(t)$

Why there exists little seasonal seasonal Y_b migration ?

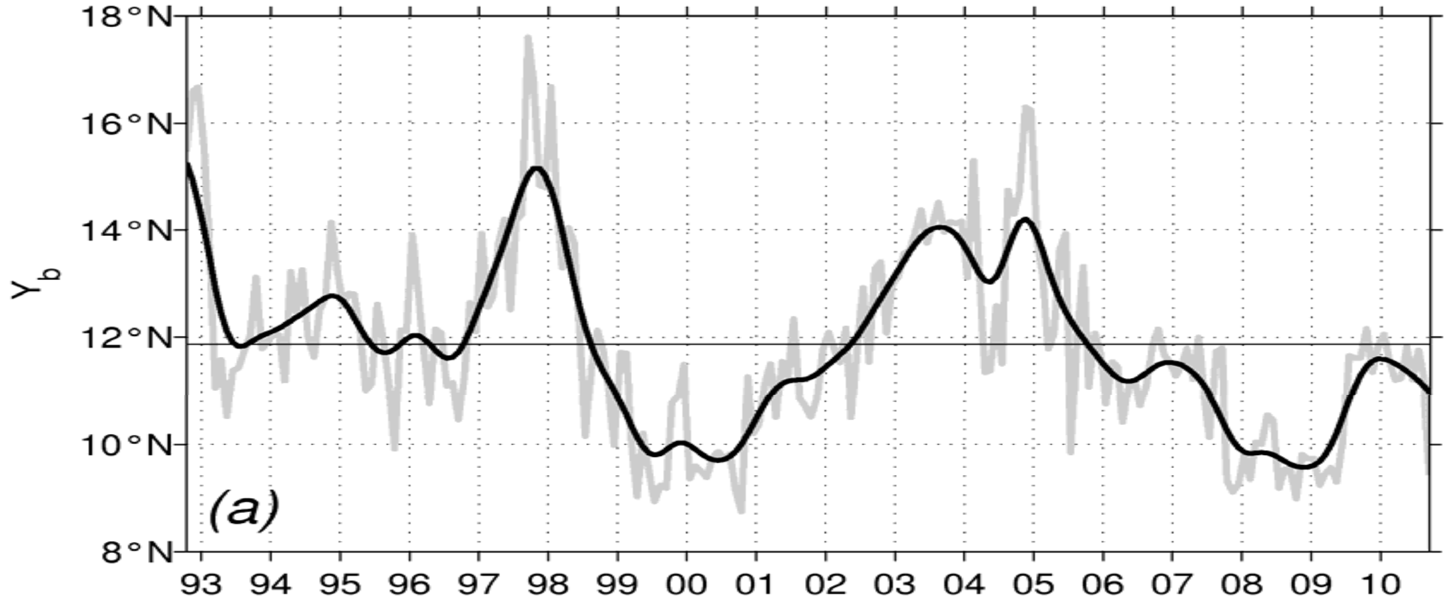

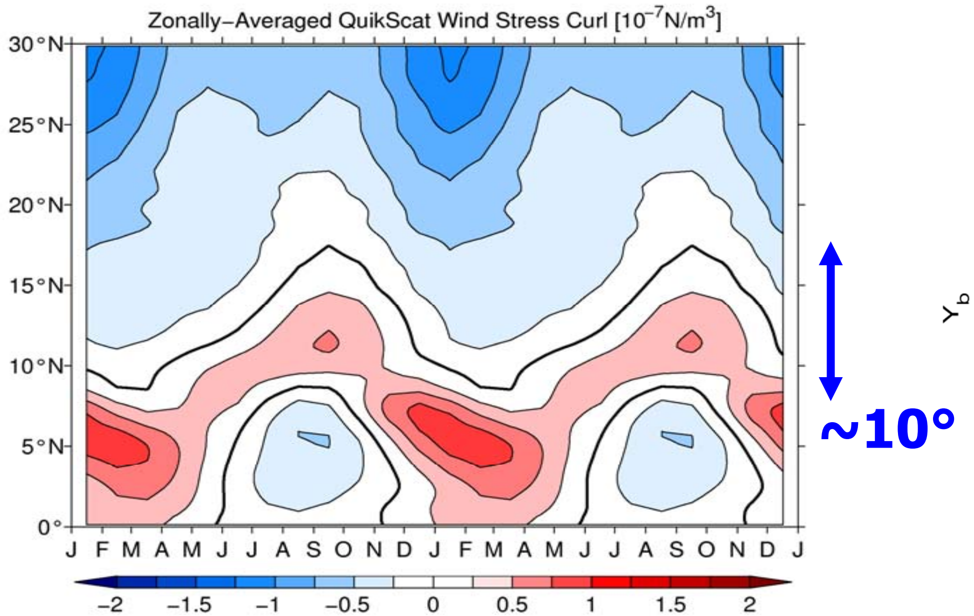

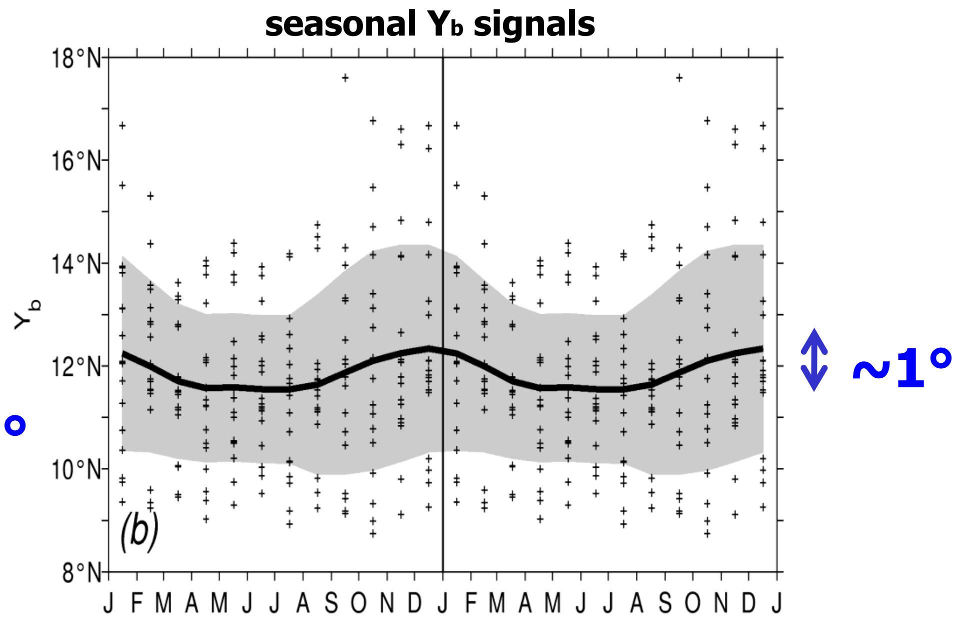

Seasonally-migrating zonal mean wind is ineffective in changing Y_b due to destructively forced signals along the wave characteristics

$$h'_m(x,y,t) = \frac{g'}{\rho_o g f}\int_{x_e}^{x} \frac{1}{c_R}\,\mathrm{curl}\,\boldsymbol{\tau}\left(x', y, t + \frac{x - x'}{c_R}\right)\exp\left[\frac{\epsilon}{c_R}(x - x')\right]dx',$$

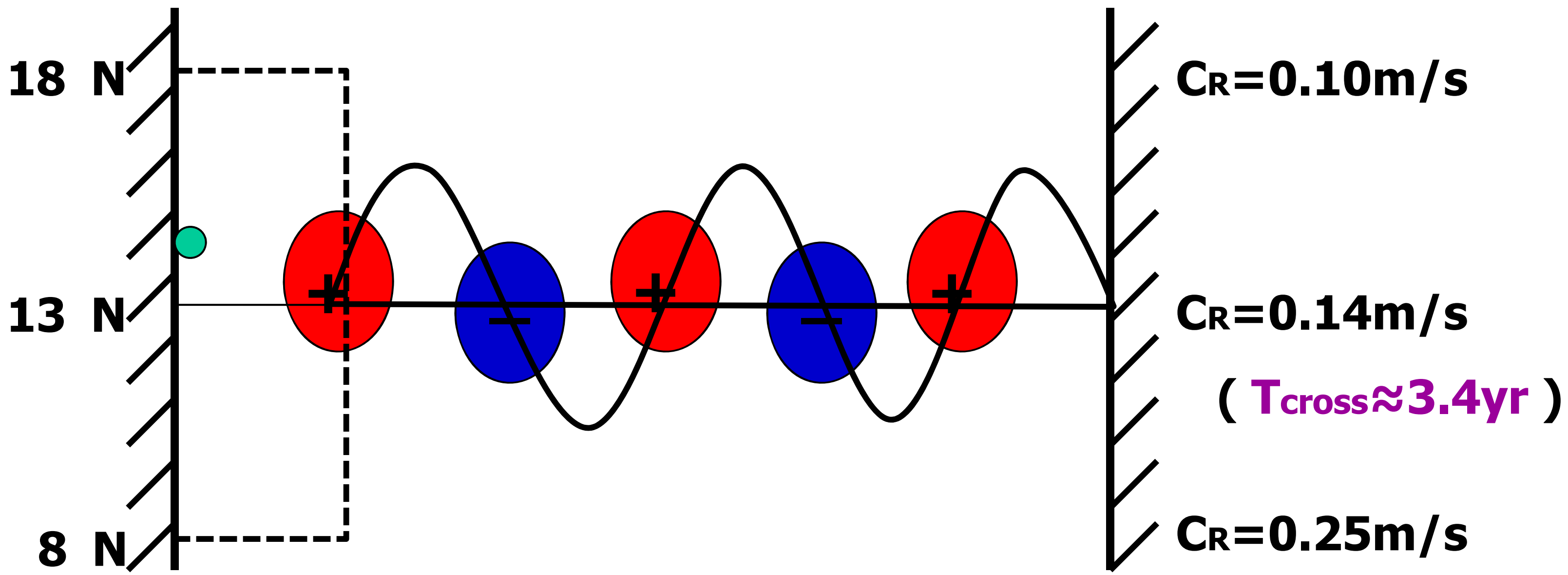

NEC bifurcation latitudes inferred from the wind-forced SSH model

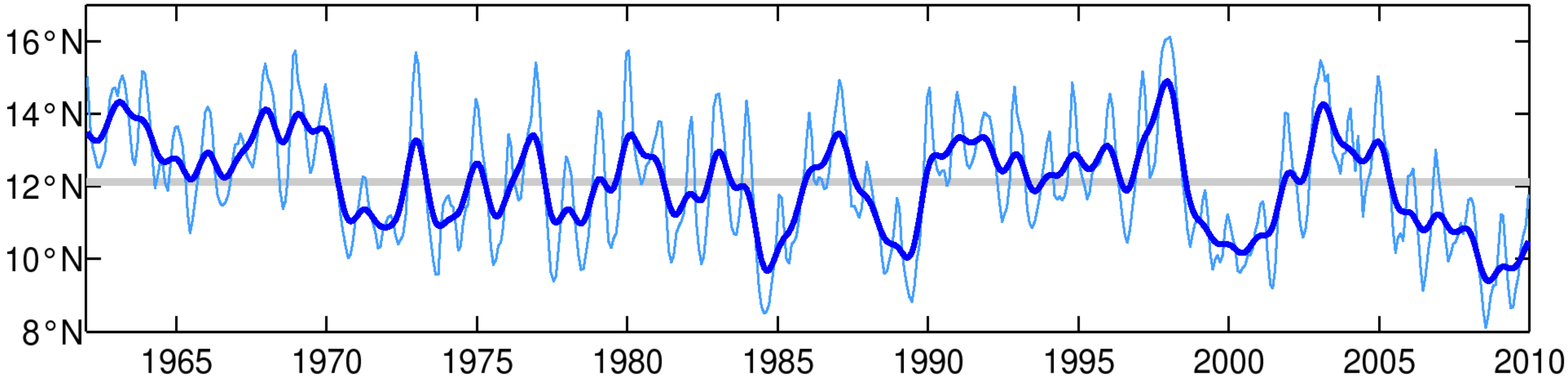

$$h'_m(x, y, t) = \frac{g'}{\rho_o g f} \int_{x_e}^{x} \frac{1}{c_R} \operatorname{curl} \boldsymbol{\tau} \left(x', y, t + \frac{x - x'}{c_R} \right) \exp \left[\frac{\epsilon}{c_R} (x - x') \right] dx',$$

c_R **: observed value**

$\operatorname{curl} \boldsymbol{\tau}$ **: monthly ECMWF reanalysis data (Balmaseda et al. 2008)**

ϵ **: Newtonian damping rate (=1/2 yrs.)**

NEC bifurcation latitudes inferred from the wind-forced SSH model

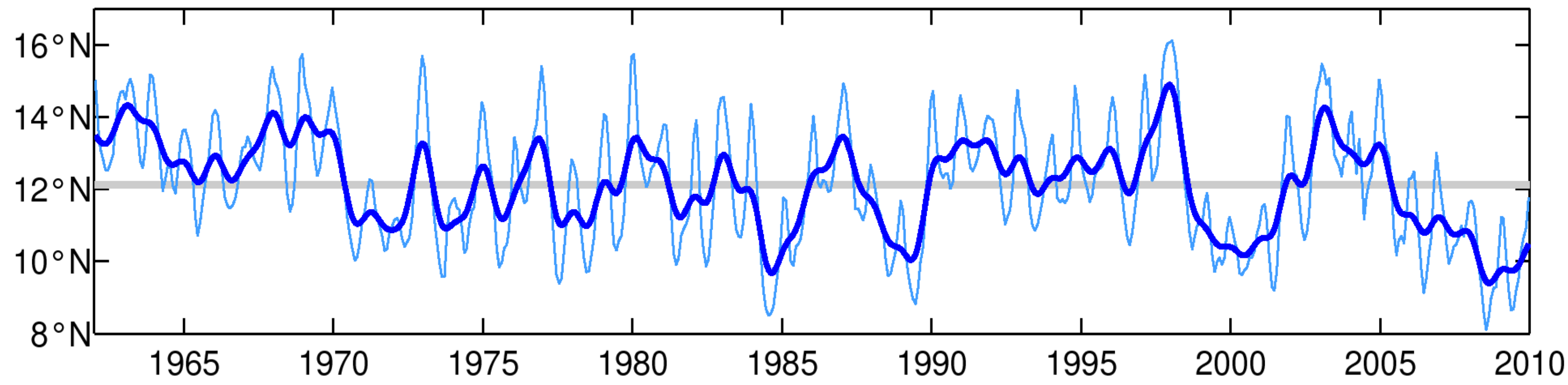

Wavelet power spectrum for $Y_m(t)$

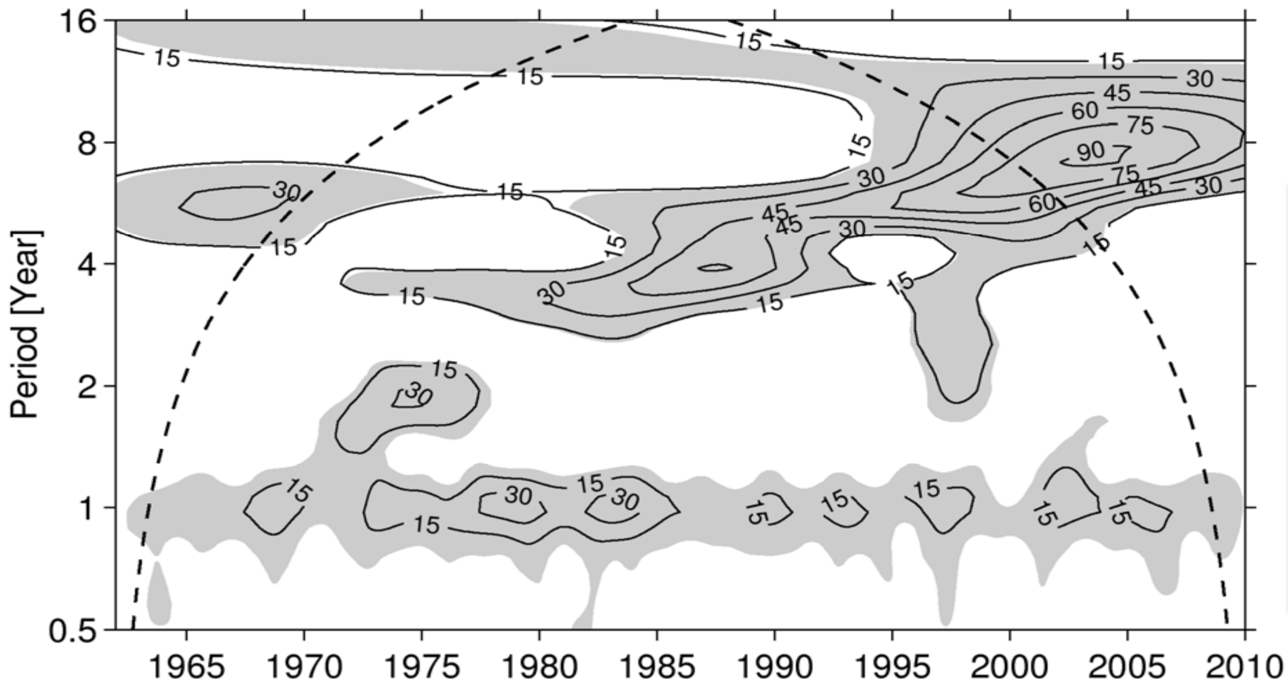

In addition to the '76/77 regime shift, there is a transition from interannual to decadal changes in NEC bifurcation after ~1993

NEC bifurcation latitudes inferred from the wind-forced SSH model

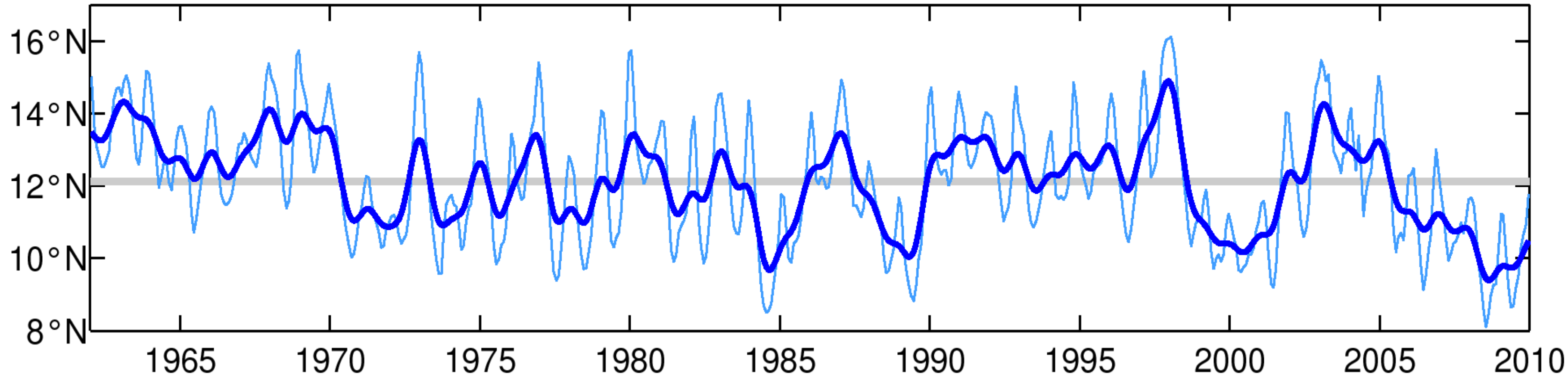

$Y_m(t)$ vs. Nino-3.4 index

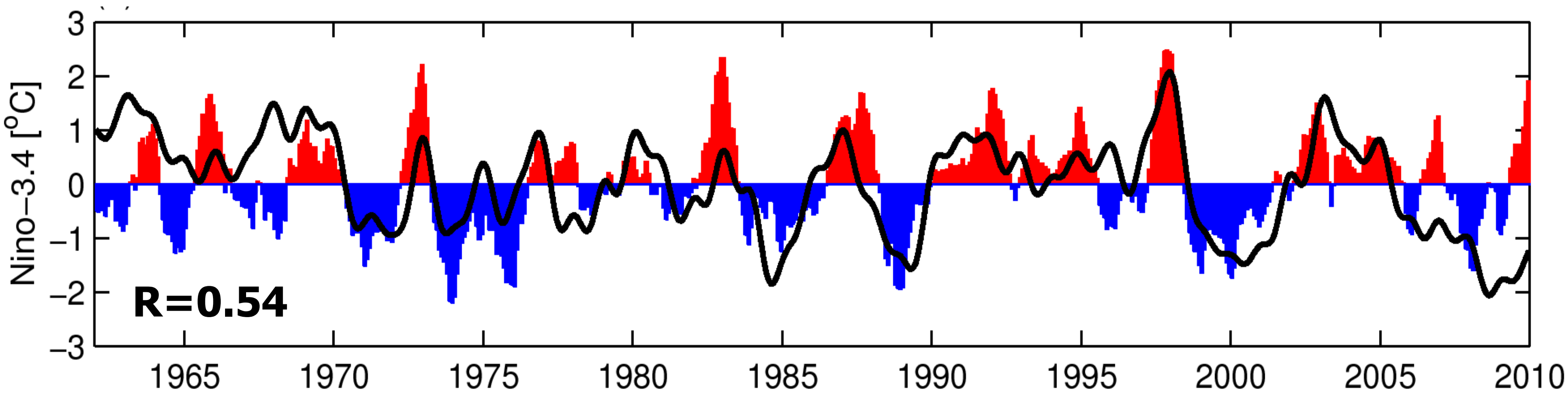

While ENSO index serves as an indicator for the time-varying NEC bifurcation, the exact $Y_b(t)$ is determined by surface wind forcing in the 12-14 N band of the western Pacific basin

Summary

- The western North Pacific LLWBC variability ranges from intra-seasonal to decadal timescales. Decadal signals dominate after 1990s.
- ENSO and regional monsoonal wind forcings are effective. Basin-scale seasonal wind has weak impact.
- Northerly bifurcation tends to coincide with El Nino, though the correspondence deteriorated in recent years.
- Wind-driven baroclinic vorticity dynamics forms an adequate framework for interannual and longer time-scale hindcast/prediction.
- Intra-seasonal variability is controlled by internal ocean dynamics (i.e. inability of removing high-PV anomalies carried by MC) and is difficult to predict.

JPO preprint: www.soest.hawaii.edu/oceanography/bo

Tropical Pacific wind stress and curl regressed to Yb(t)

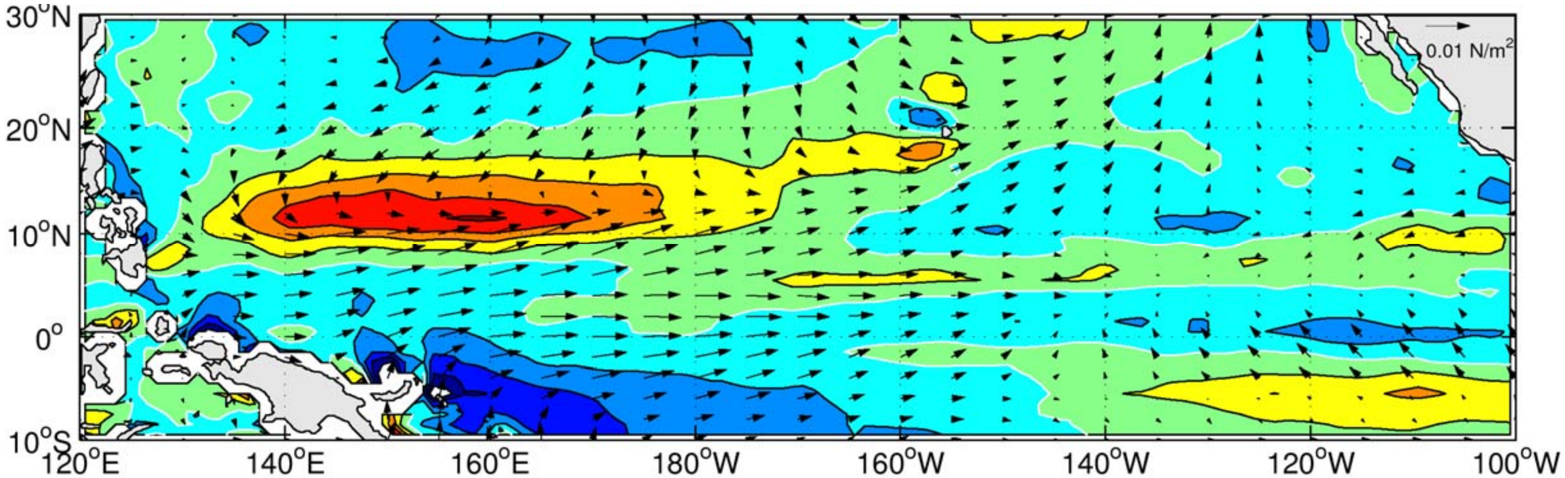

Tropical Pacific wind stress and curl regressed to Nino-3.4 index

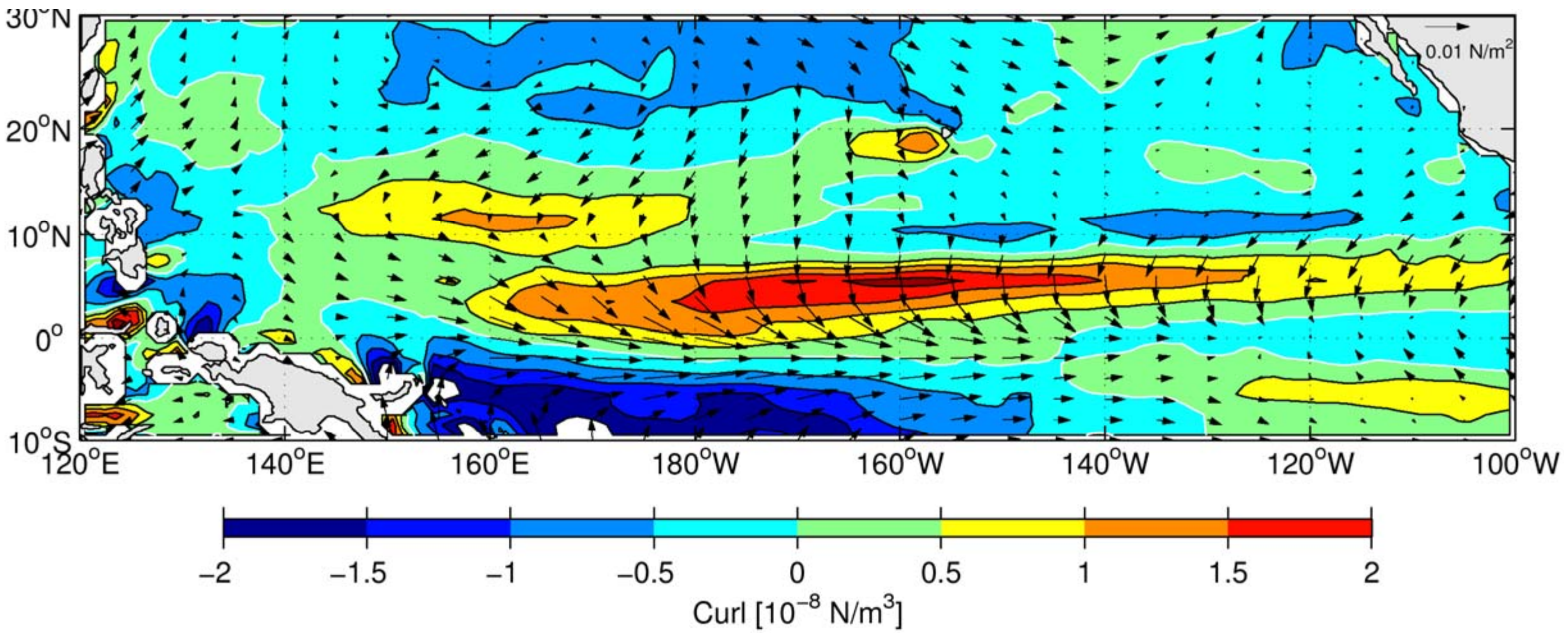

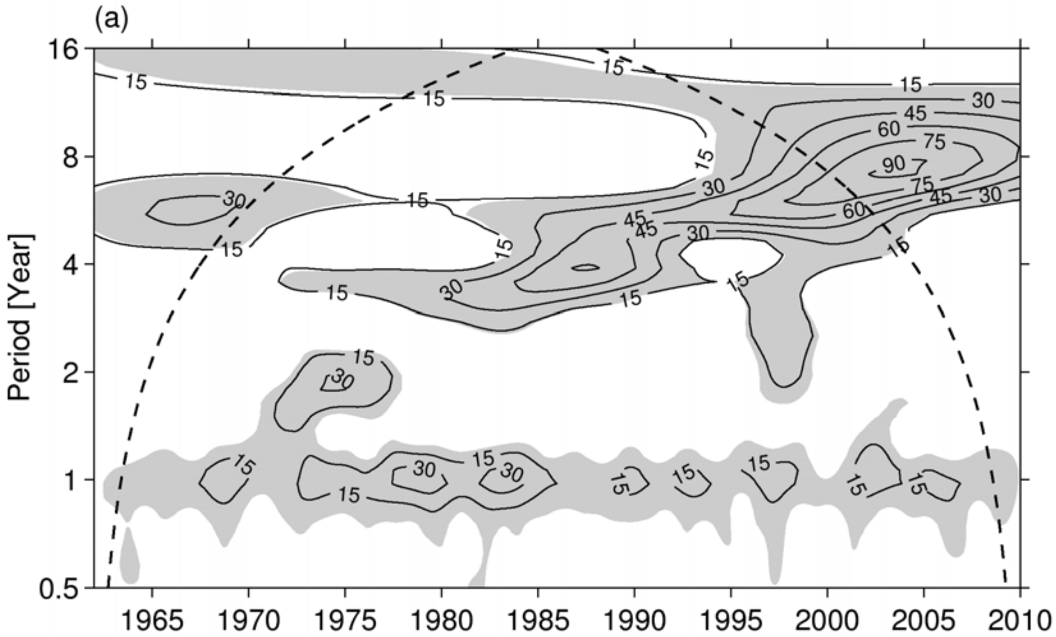

Wavelet power spectrum for model-inferred bif. latitude

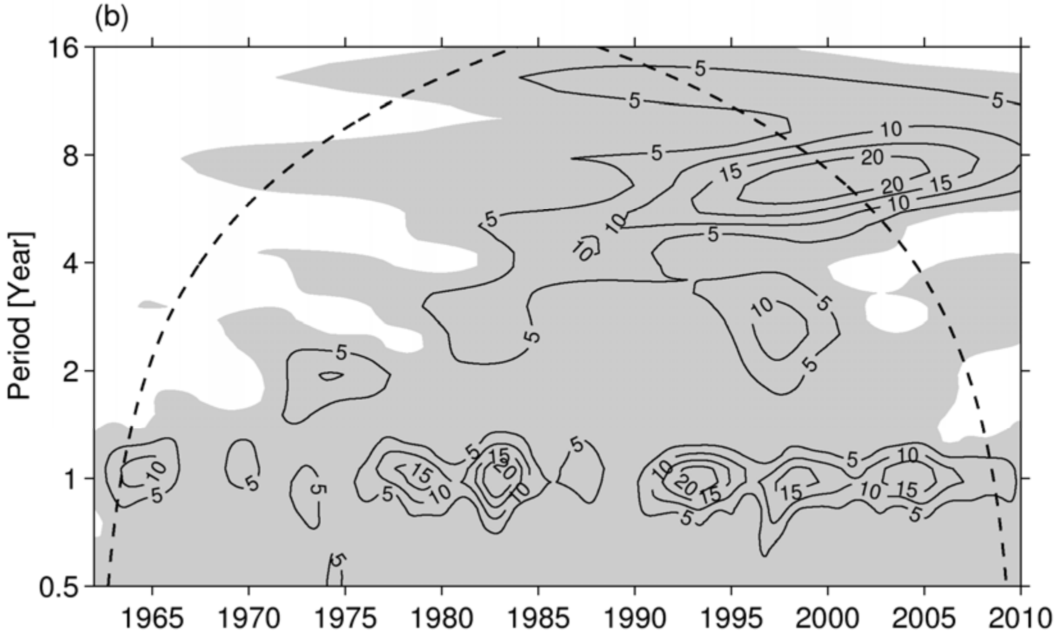

Wavelet power spectrum for wind stress curl forcing in 12°-14°N and 140°-170°E

Enhanced decadal Y_b variability after 1993 reflects the corresponding changes in wind forcing in the western Pacific